Inflammasome activation in the hip synovium of rapidly destructive coxopathy patients and its relationship with the development of synovitis and bone loss

Shunichi Yokota[1], Tomohiro Shimizu[1*], Gen Matsumae[1], Taku Ebata[1], Hend Alhasan[1], Daisuke Takahashi[1], Mohamad Alaa Terkawi[1*], Norimasa Iwasaki[1]

[1]Department of Orthopedic Surgery, Faculty of Medicine and Graduate School of Medicine, Hokkaido University, Kita-15, Nish-7, Kita-ku, Sapporo, 060-8638, Japan.

Running head: Involvement of inflammasome in RDC.

***Corresponding author**

Tomohiro Shimizu, Department of Orthopaedic Surgery, Faculty of Medicine and Graduate School of Medicine, Hokkaido University, Kita-15, Nishi-7, Kita-ku, Sapporo 060-8638, Japan. Telephone: +81-11-706-5935, Fax: +81-11-706-6054.

E-mail: simitom@wg8.so-net.ne.jp

Mohamad Alaa Terkawi, Department of Orthopaedic Surgery, Faculty of Medicine and Graduate School of Medicine, Hokkaido University, Kita-15, Nishi-7, Kita-ku, Sapporo, Japan. Telephone: +81-11-706-5935, Fax: +81-11-706-6054.

E-mail: materkawi@med.hokudai.ac.jp

Conflicts of Interest and Source of Funding: No conflicts of interest with the research.

Acknowledgment

This work was supported by research grants from Japan Society for the Promotion of Science (Grant-in-Aid for Early-Career Scientists; 20K17984) and research grants from The Uehara Memorial Foundation.

Abstract

Rapidly destructive coxopathy (RDC), a rare disease of unknown etiology, is characterized by the rapid destruction of the hip joint. In this study, the potential involvement of inflammasome signaling in the progression of RDC was investigated. Histopathological changes and the gene expression of inflammasome activation markers in hip synovial tissues collected from RDC patients was evaluated and compared to these of OA and ONFH patients. The synovial tissues of RDC patients exhibited remarkable increases in the number of infiltrated macrophages and osteoclasts, and the expression of inflammasome activation markers was also increased compared to these of OA and ONFH patients. To further understand the histopathological changes in the joint, a co-culture model of macrophages and synoviocytes was developed that mimic the joint environment. Remarkably, the gene expression of *NLRP3, GSDMD, IL-1β, TNF-α, ADMTS4, ADMTS5, MMP3, MMP9,* and *RANKL* were significantly elevated in the synoviocytes that was co-cultured with activated THP-1 macrophages suggesting the association between synovitis and inflammasome activation. Consistent with these findings, osteoclast precursor cells that were co-cultured with stimulated synoviocytes exhibited an increased number of TRAP-positive cells, compared to cells that were co-cultured with non-stimulated synoviocytes. Our findings suggest that the activation of

41 inflammasome signaling in the synovium results in an increase in local inflammation and

42 osteoclastogenesis, thus leading to the rapid bone destruction in RDC.

43 **Introduction**

44 RDC is a rare disease with an unknown etiology that was first reported in 1970. The
45 disease is characterized by the rapid deterioration of both the femoral head and the
46 acetabulum of the hip joint, which occurs within 6-12 months [1]. Clinical symptoms,
47 mainly pain, starts in the early stage when the hip appears to be radiographically normal,
48 and the symptoms increase with advancing joint destruction which is accompanied by
49 the disappearance of both femoral head and acetabulum. However, a magnetic resonance
50 imaging (MRI) examination in an early stage of the disease shows evidence of signal
51 strength abnormality for the only femoral aspects. The progression of the hip joint leads
52 to leg shortening which is accompanied by severe pain and limitations of daily life
53 activities [2]. At this stage, preservative treatment cannot solve the problem and total hip
54 arthropathy (THA) is the only option for treatment [3].

55 Despite the fact that the pathophysiology of RDC is not clear and remains to be
56 investigated, subchondral insufficiency fracture (SIF) of the femoral head has been
57 proposed as an onset of the pathology of RDC, which is consistent with features of MRI
58 in the early stage, and other mechanical factors, including, an increased pelvic inclination,
59 crystal deposition, and hip idiopathic chondrolysis has also been linked to the etiology of
60 RDC [4, 5]. Moreover, there is an emerging body of evidence to indicate that the
61 development of inflammation in the synovium is involved in the pathology of RDC [6]. In

62 line with these findings, the radiographic features of RDC are typified by rapid bone
63 resorption that occurs in both the femoral head and the acetabulum and are analogous to
64 the progressive inflammatory osteolysis that is associated with septic arthritis and
65 rheumatoid arthritis (RA) [7, 8]. Likewise, in other related diseases including osteoarthritis
66 (OA) and osteonecrosis of the femoral head (ONFH), synovial inflammation (synovitis)
67 is involved in degenerative changes in the surrounding tissues, including cartilage and
68 subchondral bone, ultimately leading to joint breakdown [9-14]. Moreover, synovitis
69 activated by inflammasome signaling has been proposed in OA, RA and gouty arthritis[15].
70 In fact, it is known that innate immune cells sense damaging by environmental factors
71 (danger signals) and trigger chronic inflammation through stimulating inflammasomes
72 and NF-κB signaling[16]. This leads to the activation of caspase-1 that facilitates the
73 subsequent cleavage and release of proinflammatory cytokines IL-1β and IL-18. Active
74 caspase-1 also triggers a unique type of cell death known as pyroptosis through cleaving
75 gasdermin D (GSDMD), which then forms a lytic pore in the plasma membrane which
76 ultimately results in the disruption of the permeability barrier of the plasma membrane
77 and the release of the intracellular contents[17]. The release of the inflammatory molecules
78 from pyroptotic cells alters the function of the synovium and impairs cartilage and bone
79 metabolism in the joint[18]. Given these facts, investigating the role of inflammasome
80 signaling in the progression of RDC represents an essential step towards developing a

81 better understanding of the pathophysiology of RDC. Such knowledge would provide
82 important clues regarding the development of therapeutic intervention strategies.
83 Given that crystal deposits and particulate debris derived from bone and cartilage tissue
84 are present in the joints of patients with SIF, they may activate damage associated
85 molecular pattern (DAMP) and inflammasome signaling in macrophages resulting in the
86 development of local chronic inflammation which would then induce bone disappearance
87 in both femoral head and the acetabulum. The objective of this study was to investigate
88 the potential involvement of inflammasome signaling in the progression of RDC. Our
89 data, using clinical samples, suggest that the inflammasome signaling pathway might be
90 involved in development of the local chronic inflammation and the bone loss that is
91 associated with joint destruction in RDC.
92

93 ## Material and Methods

94 **Patients**

95 This study was conducted in accordance with the ethical standards of our institutional
96 review board (020-0059). All patients were informed about this study and agreed to its
97 publication. In this study, a total of 218 patients who had symptomatic OA or ONFH or
98 RDC and had undergone THA from September 2018 to March 2021 were selected (Fig.1).
99 Out of 136 OA patients, 110 cases were excluded including these after osteotomy (n = 7)

100 and femoral shortening osteotomy (n = 4), subjects classified as Kellgren and Lawrence
101 (KL) grade 4 cases (N=90), and 9 other cases who declined to participate in the research.
102 For ONFH patients, a total 16 cases were excluded including subjects with bilateral hips
103 (n = 4), subjects after osteotomy (n = 4), who had no sign of synovitis (n = 4), and others
104 who declined to participate in the research (n = 4). A total 12 RDC patients were enrolled
105 in this study. Thus, a total of 64 patients of OA (n = 26), ONFH (n = 26), and RDC (n =
106 12) were investigated. Demographics data for the patients, including diagnosis, age, sex,
107 body mass index (BMI), history of corticosteroid intake, alcohol abuse, and smoking,
108 were obtained from their medical records (Table 1). Areal bone marrow density (BMD)
109 in the lumbar spine (LS, L2–L4) and femoral neck were assessed by dual-energy X-ray
110 absorptiometry (DXA; Discovery A, Hologic Japan, Inc, Tokyo, Japan).

111 **Blood samples**

112 Blood samples were obtained from fasting patients before surgery to examine the
113 biochemical markers for bone turnover related to osteoporosis, including the levels of
114 intact type 1 procollagen-N-propeptide (P1NP) and tartrate-resistant acid phosphatase 5b
115 (TRACP 5b), the inflammatory indicators, including white blood cells (WBC), CRP, and
116 HbA1c which reflect blood glucose levels over periods of months. Thereafter, blood
117 samples were centrifuged at 3000 × g at 4°C for 30 min, and serum was aliquoted and
118 stored at −80 °C for further examination.

119 **Synovial tissues and immunohistochemically staining**

120 Synovial tissues were collected from the hip joints of OA, ONFH and RDC patients
121 who were undergoing THAs. Tissues from inflamed synovial membranes were selected
122 according to standardized macroscopic criteria [19]. Synovial tissues were fixed with
123 formalin, embedded in paraffin, and then sectioned into 3-μm-thick slices for staining
124 with hematoxylin and eosin (HE, Wako, Tokyo, Japan). These specimens were stained
125 using a stain for Tartrate-Resistant Acid Phosphatase (TRAP, Wako) [20], and antibodies
126 targeting CD68 (Dako Agilent, Santa Clara, USA), NF-κB p65 (Sigma-Aldrich, Saint
127 Louis, USA), NLRP3 (Novus Biologicals, Centennial, USA), and GSDMD (Cell
128 signaling, Danvers, USA). Signals were amplified with horseradish peroxidase (HRP)-
129 conjugated streptavidin specific antibodies followed by counterstaining with hematoxylin.

130 **Synoviocytes isolation from synovial tissues**

131 Synovial tissues that were collected from the hip joints of OA, ONFH and RDC patients
132 were minced and digested with a 1% trypsin EDTA solution (GE Healthcare, Chicago,
133 USA) at 37℃-water bath for 30 min to isolate the synoviocytes. Isolated cells were
134 washed with phosphate-buffered saline (PBS), resuspended in growth medium containing
135 α-Modification minimum essential medium (α-MEM) supplemented with 10% fetal
136 bovine serum (FBS), 1% penicillin/streptomycin (PS), and 1% L-Glutamine (L-Glu) and
137 cultured in 75 cm^2 culture flasks (Costar, Cambridge, MA, USA) at 37°C in a humidified

138 5% CO2 for 5 days. Cultures were replenished with fresh medium on a daily basis and
139 each time the adherent cells were washed twice with ice-cold PBS. Adherent cells were
140 harvested after 5 days by treatment with a 1% trypsin EDTA solution for 5 min and then
141 washed 3 times with ice-cold PBS. Cell were counted and 1×10^5 cells were placed in
142 Eppendorf tubes for RNA extraction and gene expression analysis. Human fibroblast-like
143 synoviocytes (hFLS) purchased from Cell Applications (Cell Applications, San Diego,
144 USA) were used as a control. For a direct synoviocyte stimulation model, hFLS were
145 maintained in growth medium to passage 3 and 1.25×10^5 cells were then seeded at a
146 density of 2.5×10^5 cells/well on a 24-well plate. Cells were stimulated by treatment with
147 lipopolysaccharide (LPS; 100 ng/ml) plus 100 mg/ml aluminum hydroxide (Alum,
148 InvivoGen, San Diego, USA) or adenosine 5'-triphosphate (ATP) 5 mM (Thermo
149 Scientific, Waltham, USA) for 3 hours. After incubation for 24 hours, hFLS were
150 harvested for gene expression analysis by qRT-PCR.

151 **Gene expression analysis by Quantitative Real-Time Polymerase Chain Reaction**
152 **(qRT–PCR)**

153 Equal number of cells were lysed using TRIzol Reagent (Invitrogen, Waltham, USA)
154 and chloroform (Wako) was added for phase separation and RNA purification. RNA was
155 purified from the aqueous layer using NucleoSpin® RNA (Takara, Shiga, Japan) and
156 reverse transcribed using a GoScriptTM reverse transcriptase kit (Promega, Madison,

157 USA). The qRT-PCR was performed by SYBR Premix Ex TaqTM II (Takara) on a
158 Thermal Cycler Dice System 2 (Takara) with the specific primers listed in Table 2. Gene
159 expression of each target gene was calculated using the $2^{\Delta\Delta}$Ct method [21].

160 **Enzyme-linked immunosorbent assay (ELISA)**

161 Serum levels of the matrix metallopeptidases-3 (MMP-3), (MMP-9), a disintegrin and
162 metalloproteinase with thrombospondin motifs (ADAMTS-5) were measured by using
163 commercial ELISA kits (R&D Systems, Minneapolis, USA) according to the
164 manufacturer's instructions. The detection limits (sensitivity) of the kits were 31.3 pg/ml
165 for MMP-3 and MMP-9, and 125 pg/ml for ADAMTS5. In addition, the level of IL-1b in
166 supernatants of hFLS cultures was measured using commercial ELISA kits (BioLegend,
167 San Diego, USA) according to the manufacturer's instructions. The detection limit of the
168 kit was 2.0 pg/ml.

169 **Immunoblotting analyses**

170 Cells were lysed on ice using RIPA lysis buffer (ATTO Tokyo, Japan) and the
171 extracted proteins were assayed using standard SDS-PAGE and Western blot analysis
172 (ATTO) procedures. Pro-IL-1β were detected with a specific antibody (Cell signaling)
173 and signals were detected by Ez WestLumi Plus (ATTO).

174 **Establishment of macrophage-synoviocyte and synoviocyte-osteoclast precursor**
175 **co-culture models**

176 Human monocytes cell line THP1 (RIKEN, Saitama, Japan) were cultured in α-MEM
177 medium containing 10% FBS, 1% PS, 1% L-Glu at 37°C in a humidified 5% CO_2
178 atmosphere. THP-1 cells were seeded at a density of 2.5×10^5 cells/well on a 24-well plate
179 and allowed to differentiate into macrophages in the same medium supplemented with by
180 5 ng/ml phorbol myristate acetate (PMA, Sigma-Aldrich) for 48h. Thereafter, washing
181 the adherent cells three times with PBS, they were pretreated with a 10 μM NLRP3
182 inflammasome inhibitor (S3680; Selleck, Houston, USA), and then stimulated for 3 hours
183 with lipopolysaccharide (LPS; 100 ng/ml) plus 100 mg/ml aluminum hydroxide (Alum,
184 InvivoGen), or 5mM ATP (Thermo Scientific). Stimulated THP-1 macrophages were
185 washed three times with ice-cold PBS and fresh growth medium was added. In parallel,
186 hFLS were maintained in growth medium to passage 3 and 1.25×10^5 cells were then
187 seeded on a 0.4 μm pore size-transwell insert and cultured in 24-well plates. Next, the
188 inserts containing hFLS were added to the stimulated THP-1 macrophages cultures and
189 incubated for 24 h. hFLS were harvested for gene expression analysis by qRT-PCR. For
190 the establishment of a synoviocyte-osteoclast precursor co-culture model, human
191 monocytes were isolated from the blood samples obtained from healthy donors and
192 cultured in α-MEM medium containing 10% FBS, 1% PS, 1% L-Glu at 37°C in a
193 humidified 5% CO_2 atmosphere for preparing osteoclast precursors [22]. Human monocytes
194 obtained from healthy donors were cultured for 3 days in the same medium supplemented

195 with 25 ng/ml of human recombinant macrophage colony-stimulating factor (MCSF,
196 Peprotech, Cranbury, USA). Next, osteoclast precursors were obtained by culturing the
197 cells in the same medium supplemented with 25 ng/ml MCSF plus a 50 ng/ml solution of
198 recombinant human nuclear factor kappa B ligand (RANKL, Peprotech) for 24h.
199 Thereafter, the osteoclast precursors cells were washed 3 times with ice-cold PBS and co-
200 cultured with stimulated hFLS prepared as for the above model for 9 days. Cultures were
201 replenished with fresh growth medium every 2 days. Differentiated cells were stained
202 using a TRAP kit (Sigma-Aldrich) according to the manufacturer's instructions, and
203 TRAP- stained cells with ≥ 3 nuclei were identified as the osteoclasts. All in vitro
204 experiments were performed in triplicate at least twice to obtain reproducible data.

205 **Statistical analysis**

206 Statistical analyses were performed using GraphPad Software (GraphPad Software Inc.,
207 La Jolla, San Diego, USA). Differences between groups based on sex and comorbidity
208 conditions were analyzed by Pearson's Chi-square test. One-way analysis of variance
209 (ANOVA) followed by Tukey's multiple-comparison procedure was used for analyzing
210 the difference among groups. The results were considered statistically significant when *
211 $p < 0.05$, ** $p < 0.01$, *** $p < 0.001$, and **** $p < 0.0001$.

212

213 **Results**

214 **Patient demographics**

215 The demographics and clinical data for the patients revealed that there was no
216 significant difference in systemic inflammation-related factors, including WBC and CRP
217 among the three diseases (Table 1). In addition, there were no remarkable features in the
218 case of the RDC patients, but there was tendency toward higher bone metabolic markers
219 including P1NP and TRACP-5b, and lower BMD in the RDC compared to the OA and
220 ONFH cases (Table 1). Levels of MMP-3, MMP-9 and ADAMTS-5 were below the
221 detection limits of the kits (data not shown). These findings are consistent with the
222 assumption that the pathogenesis of RDC is likely dependent on local changes in the hip
223 joint, including the development of inflammation and RDC is likely dependent on local
224 changes in the hip joint, including the development of inflammation and bone fragility.

225 **Detection of inflammatory macrophages and TRAP positive cells in RDC synovial**
226 **tissues**

227 To understand the pathological processes occurring in the RDC hip, synovial tissues
228 were histologically examined, and the changes were compared to these in the OA and
229 ONFH patients. Of note, tissue-derived particulate debris from bone or cartilage was
230 observed only in the synovial tissues of the RDC patients (Fig. 2A). An increased
231 infiltration of mononuclear cells was noted in all samples, indicating the occurrence of
232 chronic inflammation (Fig. 2A). However, a remarkable increase in the level of NF-κB^{+}

233 cells was observed in the synovium in the RDC cases as compared to these for the OA
234 and ONFH patients, suggesting that advanced inflammation had occurred in these
235 samples (Fig. 2B). Given the fact that chronic inflammation promotes osteoclastogenesis,
236 synovial tissues were stained with TRAP for the detection of differentiated osteoclasts.
237 Interestingly, $TRAP^+$ multinucleated cells were present in the synovial tissues of all RDC
238 patients, but not in the synovial tissues of the OA and ONFH patients (Fig. 2B). The
239 number of NF-κB^+ cells and $TRAP^+$ multinucleated cells was also quantified in 4 clinical
240 samples for each disease. The numbers of these cells were significantly increased in the
241 RDC synovial tissues as compared to these for the OA and ONFH patients (Fig. 2C).

242 **Detection of inflammasome activation markers in RDC synovial tissues**

243 Given the fact that the presence of bone/cartilage particulate debris in the synovial
244 tissues of RDC patients that may trigger danger signals in infiltrated macrophages leading
245 to chronic inflammation, the expression of inflammasome activation markers including
246 NLRP3, NF-κB, GSDMD was further examined in synovial tissues. It is noteworthy that
247 RDC synovial tissues exhibited a higher expression of all these markers than the OA and
248 ONFH patients, in which the majority of $NLRP3^+$/$GSDMD^+$ cells were $CD68^+$ cells (Fig.
249 3A). Moreover, most of the synoviocytes were stained by an NLRP3 antibody suggesting
250 that the activation of inflammasomes had occurred in these cells (Fig. 3A). More
251 importantly, RDC synovial tissues exhibited a significant increase in the number of

252 NLRP3^{+} cells and GSDMD^{+} cells as well as CD68^{+} cells as compared to these in the OA
253 and ONFH patients (Fig. 3B). These results indicate that synovial tissues from RDC
254 patients exhibited a unique histological feature that was typified by an increase in local
255 inflammation which was accompanied by the activation of inflammasome signaling in
256 macrophages and synoviocytes, and osteoclastogenesis, which may reflect the
257 pathogenesis of the disease. To confirm the findings that point to an association between
258 the pathology of RDC and increased inflammasome activation, synoviocytes were
259 isolated from synovial tissues of patients and subjected to a gene expression analysis. The
260 expression of inflammasome activation markers, including *NLRP3, GSDMD*, and *IL-1β*
261 in synoviocytes of RDC patients was found to be significantly higher than these of healthy
262 donors or OA and ONFH patients. Consistent with this finding, these cells exhibited an
263 elevation in the expression of markers for synovial inflammation and osteoclastogenesis,
264 including *TNF-α, MMP3, MMP9* and *RANKL* (Fig. 4). These collective findings suggest
265 that the presence of bone/cartilage particulate debris in synovial tissues of RDC patients
266 might trigger inflammasome activation in macrophages and synoviocytes, resulting in the
267 production of inflammatory and osteoclastogenic cytokines being maintained, thus
268 leading to the disappearance of the femoral head and acetabulum.

269 **Association between inflammasome activation and osteoclastogenesis**

270 To test the supposition that the activation of NLRP3 inflammasomes in
271 macrophages promotes the production of inflammatory and osteoclastogenic cytokines
272 by synoviocytes, a co-culture model was developed that allows the interaction between
273 these cells to proceed. THP1 cell line macrophages were stimulated with LPS and Alum
274 or ATP to activate inflammasomes, and then co-cultured with hFLS for 24hr. Consistent
275 with the results for the clinical synovial samples, the gene expression of *NLRP3, GSDMD,*
276 *IL-1β, TNF-α, ADMTS4, ADMTS5, MMP3, MMP*9, and *RANKL* were significantly
277 elevated in the hFLS that were co-cultured with activated THP-1 and the hFLS stimulated
278 directly without co-culture (Fig. 5A & Supplementary Figure 1). Likewise, these cells
279 exhibited a significant increase in the expression of *CASP1, CASP4* and *CASP5* which
280 was accompanied by elevated levels of secreted IL-1β, but not pro-IL-1β (Fig. 5A, B),
281 suggesting the activation of canonical and non-canonical inflammasome pathways. To
282 gain further additional evidence supporting these findings, THP-1were pretreated with
283 S3680, a specific NLRP3 inflammasome inhibitor prior to being exposed to the
284 inflammasome activator and then co-cultured with hFLS. Of note, pretreatment with the
285 inflammasome inhibitor tended to reduce the expression of inflammatory cytokines and
286 inflammasome related factors (Supplementary Figure 2), which suggests that
287 synoviocytes may play a role as an inflammation amplifier in RDC. Furthermore, an in
288 vitro co-culture model was established to examine the effects of stimulated hFLS on the

289 differentiation of osteoclasts. Interestingly, the number of TRAP positive cells was
290 increased in human osteoclast precursor cell cultures that had been co-cultured with
291 stimulated hFLS as compared with these that had been co-cultured with non-stimulated
292 hFLS (Fig. 6). These results revealed that inflammasome activation in the synovium
293 promotes synovitis and osteoclast differentiation in the joint.
294

295 **Discussion**

296 The inability to therapeutically prevent joint destruction in RDC is likely due to our
297 incomplete understanding of the disease pathophysiology. Despite the accumulating
298 evidence suggesting that SIF and inflammation are the main etiological factors, our
299 overall knowledge of the mechanism responsible for RDC remains to be achieved [4, 6, 23].
300 In the current study, the association between inflammasome activation and the
301 development of synovitis and bone disappearance was investigated in RDC. The
302 histopathological changes and gene expression of inflammasome activation markers in
303 the synovium of RDC patients were initially studied and the results compared with those
304 of clinically related hip diseases of OA and ONFH. A co-culture model that mimics the
305 joint environment was then developed in an attempt to explore the impact of
306 inflammasome activation in macrophages and synoviocytes on the progression of
307 synovitis and bone disappearance.

308 The current findings revealed that RDC synovium exhibited unique histological
309 features that were clearly different from these in OA and ONFH joints as typified by an
310 elevation in the infiltrated macrophages and osteoclasts. Moreover, synoviocytes from
311 RDC patients expressed greater levels of inflammasome activation markers,
312 proinflammatory cytokines and matrix metalloproteinases that are all involved in the
313 development of a high grade of synovitis and bone loss. Such changes provide a possible
314 explanation for the rapid disappearance of femoral and acetabular bone in RDC patients
315 despite the deterioration of only the femoral aspect in its early stage [1]. In a previous report,
316 the pathogenesis of OA was characterized by changes in the articular cartilage and the
317 formation of osteophytes and sclerosis over a period of several years [12], while in ONFH,
318 changes occur in the femoral head, thus leading to the progressive collapse of the femoral
319 head, not acetabulum, within several years, a substantially shorter time [13, 14]. In line with
320 these findings, numerous reports have underlined the correlation between the grade of
321 synovitis and the speed of deterioration of the hip joint [24, 25].

322 It should also be noted that the histological features observed in the synovium in
323 RDC patients were analogous to features in rheumatoid and septic arthritis. These include
324 an increase in infiltrated inflammatory macrophages and osteoclasts as well as the
325 presence of particulate debris derived from bone or cartilage [26, 27]. However, in contrast
326 to rheumatoid arthritis, the levels of pro-inflammatory markers in the blood were not

327 evident in RDC patients, but only bone metabolic markers. In some previous case reports,
328 RDC patients were reported to show elevated levels of C-reactive protein and
329 inflammatory cytokines, which was accompanied by an increase in white blood cell
330 count[28 29]. Nonetheless, it is known that RDC is characterized by local pathological
331 changes in a single joint and the increase of systemic inflammatory markers might be
332 nonspecific and influenced by the progression of other diseases and anti-inflammatory
333 treatment. It should also be noted that the majority of clinical studies showed an
334 association between RDC and elevated bone metabolic markers in blood samples of
335 patients [30-32]. The most important finding in the current study is the elevation in markers
336 for the expression of inflammasome activation in the synovium of the hips of RDC
337 patients. Inflammasomes are intracellular multiprotein signaling platforms that are
338 dependent on the enzymatic activity of caspase-1 that activates the cleavage of GSDMD,
339 which, in turn, produces a pore-like structure in the cell membrane leading to the
340 formation of pyroptotic cells followed by the release of proinflammatory cytokines. The
341 activation of inflammasomes in the synovium of RDC patients is most likely initiated by
342 SIF and is accompanied by the deposition of damaged tissue in the synovium, whereas
343 innate immune cells, including macrophages sense and phagocytize these substances
344 resulting in the activation of NLRP3 signaling. The prolonged activation of NLRP3
345 results in an increase in the number of pyroptotic cells in the synovium, a condition that

346 promotes the rapid proliferation and stimulation of synoviocytes. In turn, stimulated
347 synoviocytes amplify inflammation and promote the development of chronic synovitis
348 that mediates osteoclastogenesis and focal bone loss thus resulting in joint destruction. In
349 line with the findings, it has been suggested that the activation inflammasomes in arthritic
350 diseases is associated with bone erosion in rheumatoid arthritis [15, 33] . Nonetheless,
351 NLRP3 inflammasome signaling appears to be associated with increased osteoclast
352 differentiation and bone resorption in a number of pathological conditions [34] . Thus, the
353 bone disappearance that is observed in RDC and RA is most probably due to a higher
354 inflammation related with inflammasome activation. Given these findings, along with
355 previous reports that bone matrix components activate the NLRP3 inflammasome and
356 promote osteoclast differentiation, it could be concluded that SIF with a higher grade of
357 inflammation response to bone matrix debris from fracture fragments of SIF, may proceed
358 with the development of RDC. In contrast, lower grade of synovial inflammation with
359 SIF would induce damage to the articular cartilage and the formation of osteophytes and
360 sclerosis over a period of several years resulting in OA. Likewise, necrotic bone matrix
361 debris from the collapse of ONFH would not induce as higher inflammation as RDC.

362 The major limitations of the present study include, the small sample size, especially
363 the number of RDC patients, and the lack of appropriate controls such as OA patients
364 resulting from SIF collapse. However, it is difficult to obtain such samples because a

365 diagnosis of SIF at the asymptomatic early stage is not possible. One more limitation, is
366 the lack of data demonstrating that the synoviocytes from clinical samples of RDC
367 patients promote osteoclast differentiation. However, the current study clearly shows that
368 synoviocytes from clinical samples express osteoclastogenic factors and that the activated
369 synoviocytes are able to promote osteoclast differentiation in vitro. Further evidence for
370 the contribution of inflammasome signaling to the pathogenesis of RDC may reveal novel
371 therapeutic intervention strategies for the treatment of RDC based on inflammasome-
372 targeted therapies.

373 In conclusion, this is the first study to report on the potential involvement of
374 inflammasome signaling in development of synovitis and osteoclastogenesis in RDC
375 patients. Our findings suggest that the occurrence of SIF with poor repair may activate
376 inflammasome signaling in the synovium resulting in an increase in local inflammation
377 and osteoclastogenesis leading to rapid bone destruction in RDC patients. A further study
378 with a larger number of samples with different stages of this disease will be required for
379 a better understanding of etiology in RDC.

380

381 **Author contributions**

382 T.S, MA.T, and N.I were involved in study conception and design: S.Y performed
383 experiments: S.Y, T.S, G.M, T.E, H.A, D.T, and MA.T were performed data analysis and

interpretation: S.Y wrote manuscript: T.S, D.T, MA.T secured research funding: MA.T, T.S, N.I performed final proofreading. T.S and MA.T are the guarantor of this work and, as such, had full access to all of the data in the study and takes responsibility for the integrity of the data and the accuracy of the data analysis.

References

[1] Postel M, Kerboull M: Total prosthetic replacement in rapidly destructive arthrosis of the hip joint. Clin Orthop Relat Res 1970, 72:138-44.

[2] Lequesne M: [Rapid destructive coxarthritis]. Rhumatologie 1970, 22:51-63.

[3] Kuo A, Ezzet KA, Patil S, Colwell CW, Jr.: Total hip arthroplasty in rapidly destructive osteoarthritis of the hip: a case series. Hss j 2009, 5:117-9.

[4] Yamamoto T, Bullough PG: The role of subchondral insufficiency fracture in rapid destruction of the hip joint: a preliminary report. Arthritis Rheum 2000, 43:2423-7.

[5] Menkes CJ, Simon F, Delrieu F, Forest M, Delbarre F: Destructive arthropathy in chondrocalcinosis articularis. Arthritis Rheum 1976, 19 Suppl 3:329-48.

[6] Abe H, Sakai T, Ando W, Takao M, Nishii T, Nakamura N, Hamasaki T, Yoshikawa H, Sugano N: Synovial joint fluid cytokine levels in hip disease. Rheumatology (Oxford) 2014, 53:165-72.

[7] Shu J, Ross I, Wehrli B, McCalden RW, Barra L: Rapidly destructive inflammatory arthritis of the hip. Case Rep Rheumatol 2014, 2014:160252.

[8] Hart G, Fehring T: Rapidly destructive osteoarthritis can mimic infection. Arthroplast Today 2016, 2:15-8.

406 [9] McAllister MJ, Chemaly M, Eakin AJ, Gibson DS, McGilligan VE: NLRP3 as a
407 potentially novel biomarker for the management of osteoarthritis. Osteoarthritis
408 Cartilage 2018, 26:612-9.
409 [10] Rabquer BJ, Tan GJ, Shaheen PJ, Haines GK, 3rd, Urquhart AG, Koch AE:
410 Synovial inflammation in patients with osteonecrosis of the femoral head. Clin Transl
411 Sci 2009, 2:273-8.
412 [11] Murphy NJ, Eyles JP, Hunter DJ: Hip Osteoarthritis: Etiopathogenesis and
413 Implications for Management. Adv Ther 2016, 33:1921-46.
414 [12] Zhao D, Zhang F, Wang B, Liu B, Li L, Kim SY, Goodman SB, Hernigou P, Cui Q,
415 Lineaweaver WC, Xu J, Drescher WR, Qin L: Guidelines for clinical diagnosis and
416 treatment of osteonecrosis of the femoral head in adults (2019 version). J Orthop
417 Translat 2020, 21:100-10.
418 [13] Kloen P, Leunig M, Ganz R: Early lesions of the labrum and acetabular cartilage in
419 osteonecrosis of the femoral head. J Bone Joint Surg Br 2002, 84:66-9.
420 [14] Jawad MU, Haleem AA, Scully SP: In brief: Ficat classification: avascular necrosis
421 of the femoral head. Clin Orthop Relat Res 2012, 470:2636-9.
422 [15] Spel L, Martinon F: Inflammasomes contributing to inflammation in arthritis.
423 Immunol Rev 2020, 294:48-62.

424 [16] Lamkanfi M, Dixit VM: Mechanisms and functions of inflammasomes. Cell 2014,
425 157:1013-22.
426 [17] Bergsbaken T, Fink SL, Cookson BT: Pyroptosis: host cell death and inflammation.
427 Nat Rev Microbiol 2009, 7:99-109.
428 [18] Hamasaki M, Terkawi MA, Onodera T, Homan K, Iwasaki N: A Novel Cartilage
429 Fragments Stimulation Model Revealed that Macrophage Inflammatory Response
430 Causes an Upregulation of Catabolic Factors of Chondrocytes In Vitro. Cartilage 2021,
431 12:354-61.
432 [19] Ayral X: Diagnostic and quantitative arthroscopy: quantitative arthroscopy.
433 Baillieres Clin Rheumatol 1996, 10:477-94.
434 [20] Blumer MJ, Hausott B, Schwarzer C, Hayman AR, Stempel J, Fritsch H: Role of
435 tartrate-resistant acid phosphatase (TRAP) in long bone development. Mech Dev 2012,
436 129:162-76.
437 [21] Ebata T, Terkawi MA, Hamasaki M, Matsumae G, Onodera T, Aly MK, Yokota S,
438 Alhasan H, Shimizu T, Takahashi D, Homan K, Kadoya K, Iwasaki N: Flightless I is a
439 catabolic factor of chondrocytes that promotes hypertrophy and cartilage degeneration
440 in osteoarthritis. iScience 2021, 24:102643.
441 [22] Terkawi MA, Kadoya K, Takahashi D, Tian Y, Hamasaki M, Matsumae G, Alhasan
442 H, Elmorsy S, Uetsuki K, Onodera T, Takahata M, Iwasaki N: Identification of IL-27 as

443 potent regulator of inflammatory osteolysis associated with vitamin E-blended ultra-
444 high molecular weight polyethylene debris of orthopedic implants. Acta Biomater 2019,
445 89:242-51.
446 [23] Shimizu T, Yokota S, Kimura Y, Asano T, Shimizu H, Ishizu H, Iwasaki N,
447 Takahashi D: Predictors of cartilage degeneration in patients with subchondral
448 insufficiency fracture of the femoral head: a retrospective study. Arthritis Res Ther
449 2020, 22:150.
450 [24] Solomon L, Schnitzler CM, Browett JP: Osteoarthritis of the hip: the patient behind
451 the disease. Ann Rheum Dis 1982, 41:118-25.
452 [25] Solomon L, Schnitzler CM: Pathogenetic types of coxarthrosis and implications for
453 treatment. Arch Orthop Trauma Surg 1983, 101:259-61.
454 [26] Mbalaviele G, Novack DV, Schett G, Teitelbaum SL: Inflammatory osteolysis: a
455 conspiracy against bone. J Clin Invest 2017, 127:2030-9.
456 [27] Allard-Chamard H, Carrier N, Dufort P, Durand M, de Brum-Fernandes AJ, Boire
457 G, Komarova SV, Dixon SJ, Harrison RE, Manolson MF, Roux S: Osteoclasts and their
458 circulating precursors in rheumatoid arthritis: Relationships with disease activity and
459 bone erosions. Bone Rep 2020, 12:100282.
460 [28] Ando W, Hashimoto Y, Yasui H, Ogawa T, Koyama T, Tsuda T, Ohzono K:
461 Progressive Bone Destruction in Rapidly Destructive Coxopathy Is Characterized by

462 Elevated Serum Levels of Matrix Metalloprotease-3 and C-Reactive Protein. J Clin
463 Rheumatol 2022, 28:e44-e8.
464 [29] Nakano S, Nakajima A, Sonobe M, Yamada M, Takahashi H, Aoki Y, Terai K,
465 Hiruta H, Nakagawa K: Rapidly destructive coxopathy due to dialysis amyloidosis: a
466 case report. Mod Rheumatol Case Rep 2021, 5:437-41.
467 [30] Ogawa K, Mawatari M, Komine M, Shigematsu M, Kitajima M, Kukita A,
468 Hotokebuchi T: Mature and activated osteoclasts exist in the synovium of rapidly
469 destructive coxarthrosis. J Bone Miner Metab 2007, 25:354-60.
470 [31] Seitz S, Zustin J, Amling M, Ruther W, Niemeier A: Massive accumulation of
471 osteoclastic giant cells in rapid destructive hip disease. J Orthop Res 2014, 32:702-8.
472 [32] Abe H, Sakai T, Ogawa T, Takao M, Nishii T, Nakamura N, Sugano N:
473 Characteristics of bone turnover markers in rapidly destructive coxopathy. J Bone Miner
474 Metab 2017, 35:412-8.
475 [33] Jin C, Frayssinet P, Pelker R, Cwirka D, Hu B, Vignery A, Eisenbarth SC, Flavell
476 RA: NLRP3 inflammasome plays a critical role in the pathogenesis of hydroxyapatite-
477 associated arthropathy. Proc Natl Acad Sci U S A 2011, 108:14867-72.
478 [34] Alippe Y, Wang C, Ricci B, Xiao J, Qu C, Zou W, Novack DV, Abu-Amer Y,
479 Civitelli R, Mbalaviele G: Bone matrix components activate the NLRP3 inflammasome
480 and promote osteoclast differentiation. Sci Rep 2017, 7:6630.

481 [35] Li Y, Huang H, Liu B, Zhang Y, Pan X, Yu XY, Shen Z, Song YH: Inflammasomes
482 as therapeutic targets in human diseases. Signal Transduct Target Ther 2021, 6:247.
483
484

485 **Figure legends**

486 **Figure 1.** Flow chart describing the clinical samples included in the current study.

487 **Figure 2.** Detection of inflammatory macrophages and $TRAP^+$ cells in synovial tissues.
488 Histological analysis of synovial tissues collected from patients diagnosed with OA,
489 ONFH and RDC patients (4 cases for each condition). A) Representative images for the
490 stained sections with HE. The arrows in the figures indicate bone debris. B)
491 Representative images of immuno-stained sections with antibodies to NF-kB, and TRAP.
492 The arrows in the figures indicate bone debris. Scale bars are 50 μm. C) Count of stained
493 cells by antibodies in sections of the tissues. Theresults represent the mean ± SEM for 4
494 samples and significant difference was determined by the One-way ANOVA, followed
495 by Tukey's multiple-comparison procedure. Significance is presented as ** $p < 0.01$ and
496 **** $p < 0.0001$.

497 **Figure 3.** Immunohistochemical detection of inflammasome activation markers in
498 synovial tissue. Histological analysis of synovial tissues collected from diagnosed OA,
499 ONFH and RDC patients (4 cases for each condition). A) Images are representative of
500 sections stained with antibodies to NLRP3, NF-kB, GSDMD, and CD68. The arrows in
501 the figures indicate bone debris. Scale bars are 50 μm. B) Quantification of stained cells
502 by antibodies in sections of the tissues. Results represent the mean ± SEM for 4 samples
503 and significant differences were determined by the One-way ANOVA, followed by

504 Tukey's multiple-comparison procedure. Significance is presented as ** $p < 0.01$, *** p

505 < 0.001, and **** $p < 0.0001$.

506 **Figure 4.** Detection of inflammasome activation and inflammatory markers in

507 synoviocytes from clinical samples by qRT-PCR. Results represent the mean ± SEM for

508 4 samples of each condition. Significant difference was determined by the One-way

509 ANOVA, followed by Tukey's multiple-comparison procedure. Significance is presented

510 as * $p < 0.05$, ** $p < 0.01$, and *** $p < 0.001$.

511 **Figure 5.** Effect of inflammasome activation in macrophages on the development of

512 inflammation mediated by synoviocytes. A) Expression of inflammatory and

513 inflammasome activation markers in hFLS co-cultured THP-1 cells that were stimulated

514 with of LPS or LPS+Alum as analyzed by qRT-PCR. Results represent the mean ± SEM

515 for triplicate experiments and significant differences was determined by the One-way

516 ANOVA, followed by Tukey's multiple-comparison procedure. B) Detection of cellular

517 and secreted IL-1β in hFLS cultured with THP-1 cells that were stimulated with LPS or

518 LPS+Alum as analyzed by Western blot analysis (left panel) and ELISA (Right panel).

519 Significance is presented as * $p < 0.05$, ** $p < 0.01$, *** $p < 0.001$, and **** $p < 0.0001$.

520 Experiments were performed at least twice in triplicates to obtain reproducible data.

521 **Figure 6.** Induction of osteoclastogenesis in an osteoclast precursor cell culture by

522 stimulated synoviocytes. A) In vitro model for co-culturing stimulated hFLS and

523 osteoclast precursors using transwell system. Stimulated hFLS promoted
524 osteoclastogenesis. B) Representative images for TRAP-stained cells. Scale bars
525 represent 100 μm. C) Quantification of $TRAP^+$ positive cells in osteoclast precursors after
526 co-culturing with stimulated FLS. Results represent the mean ± SEM of triplicates
527 experiments and significant differences were determined by the Student's t-test.
528 Significance is presented as * $p < 0.05$. Experiments were performed at least twice in
529 triplicates to obtain reproducible data.
530
531
532
533
534
535
536
537
538
539
540
541
542

543 Table 1. Demographics of clinical population.

	OA (N = 26)	ONFH (N = 26)	RDC (N = 12)	OA vs ONFH	ONFH vs RDC	OA vs RDC
Age (years)	66.8±1.8	54.4±2.4	75.0±2.5	p<0.001	p<0.001	p=0.075
Sex M:F	8:20	12:14	5:7	p=0.080	p=0.080	p=0.240
BMI (kg/m^2)	27.2±0.93	24.3±0.87	22.0±0.90	p=0.030	p=0.353	p=0.003
P1NP (mg/mL)	52.5±5.6	46.4±7.0	94.2±16	p=0.821	p<0.001	p=0.005
TRACP-5b (mU/dL)	457±32	424±41	564±47	p=0.117	p=0.006	p=0.233
WB (Cell/mL)	6050±326	7135±414	6250±733	p=0.140	p=0.429	p=0.957
CRP (mg/dL)	0.13±0.03	0.35±0.16	0.38±0.11	p=0.338	p=0.988	p=0.414
HbA1c %	6.1±0.15	5.5±0.10	5.7±0.13	p=0.004	p=0.556	p=0.248
BMD(L) (g/cm^2)	1.01±0.04	0.90±0.04	0.81±0.05	p=0.170	p=0.337	p=0.015
BMD(FN) ($g/cm^{2)}$	0.73±0.03	0.72±0.04	0.60±0.04	p=0.983	p=0.150	p=0.121
Hypertensioin	17 (65.4%)	2 (7.7%)	5 (41.7%)	p<0.001	p=0.012	p=0.169
Hyperlipidaemia	10 (38.5%)	1 (3.9%)	3 (25.0%)	p=0.048	p<0.001	p=0.416
Diabetes mellitus	9 (37.5%)	1 (10%)	1 (8.3%)	p=0.003	p=0.565	p=0.065
Thyroid disease	5 (19.2%)	2 (7.7%)	1 (8.3%)	p=0.223	p=0.946	p=0.392
Steroid	7 (26.9%)	21(80.8%)	1 (8.3%)	p<0.001	p<0.001	p=0.191
Alcohol abuse	4 (15.4%)	9 (34.6%)	2 (16.7%)	p=0.109	p=0.256	p=0.920
Smoking	9 (37.5%)	18(69.2%)	6 (50.0%)	p=0.025	p=0.253	p=0.473

544

545

546

547

548

549 Table. 2. Primers used for qRT-PCR.

Target	Forward	Reverse
β–actin	5’-CCTCACCCTGAAGTACCCA-3’	5’-TCGTCCAGTTGGTGACGAT-3’
IL-1β	5’-GCAGAAGTACCTGAGCTCGC-3’	5’-ATAGCAAATCGGCTGACGGT-3’
TNF-α	5’-GCCCATGTTGTAGCAAACCC-3’	5’-TATCTCTCAGCTCCACGCCA-3’
NLRP3	5’-AGAAGCTCTGGTTGGTCAGC-3’	5’-GAGTCTGGTCAGGAATGGC-3’
GSDMD	5’-GCTCCATGAGAGGCACCTG-3’	5’-TTCTGTGTCTGCAGCACCTC-3’
MMP-3	5’-TCCTACTGTTGCTGTGCGTG-3’	5’-CCCTTGCAGCTCCATCCAAT-3’
MMP-9	5’-GTACTCGACCTGTACCAGCG-3’	5’-AGAAGCCCCACTTCTTGTCG-3’
ADAMTS4	5’-CAGTCAGGCTCCTTCAGGAAA-3’	5’-TGCTGCCGGACAAGAATGTG-3’
ADAMTS5	5’-CCAGGATCTGCTTTCGTGGT-3’	5’-TCCAAATGCACTTCAGCCAC-3’
RANKL	5’-ATCTGGCCAAGAGGAGCAAG-3’	5’-GGGAACCAGATGGGATGTCG-3’

550

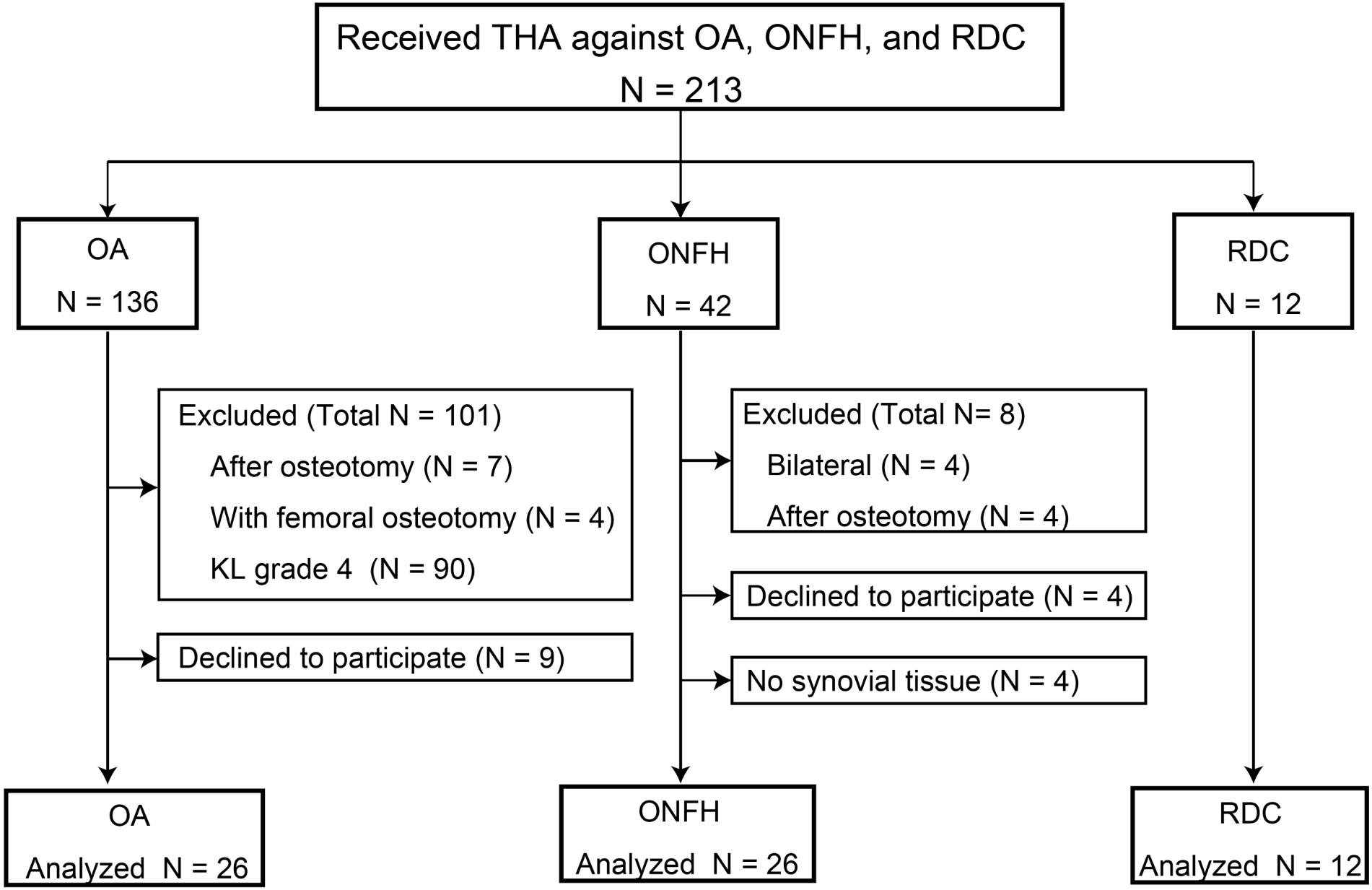
Received THA against OA, ONFH, and RDC
N = 213
OA
N = 136
ONFH
N = 42
RDC
N = 12
Excluded (Total N = 101)
After osteotomy (N = 7)
With femoral osteotomy (N = 4)
KL grade 4 (N = 90)
Declined to participate (N = 9)
Excluded (Total N= 8)
Bilateral (N = 4)
After osteotomy (N = 4)
Declined to participate (N = 4)
No synovial tissue (N = 4)
OA
Analyzed N = 26
ONFH
Analyzed N = 26
RDC
Analyzed N = 12

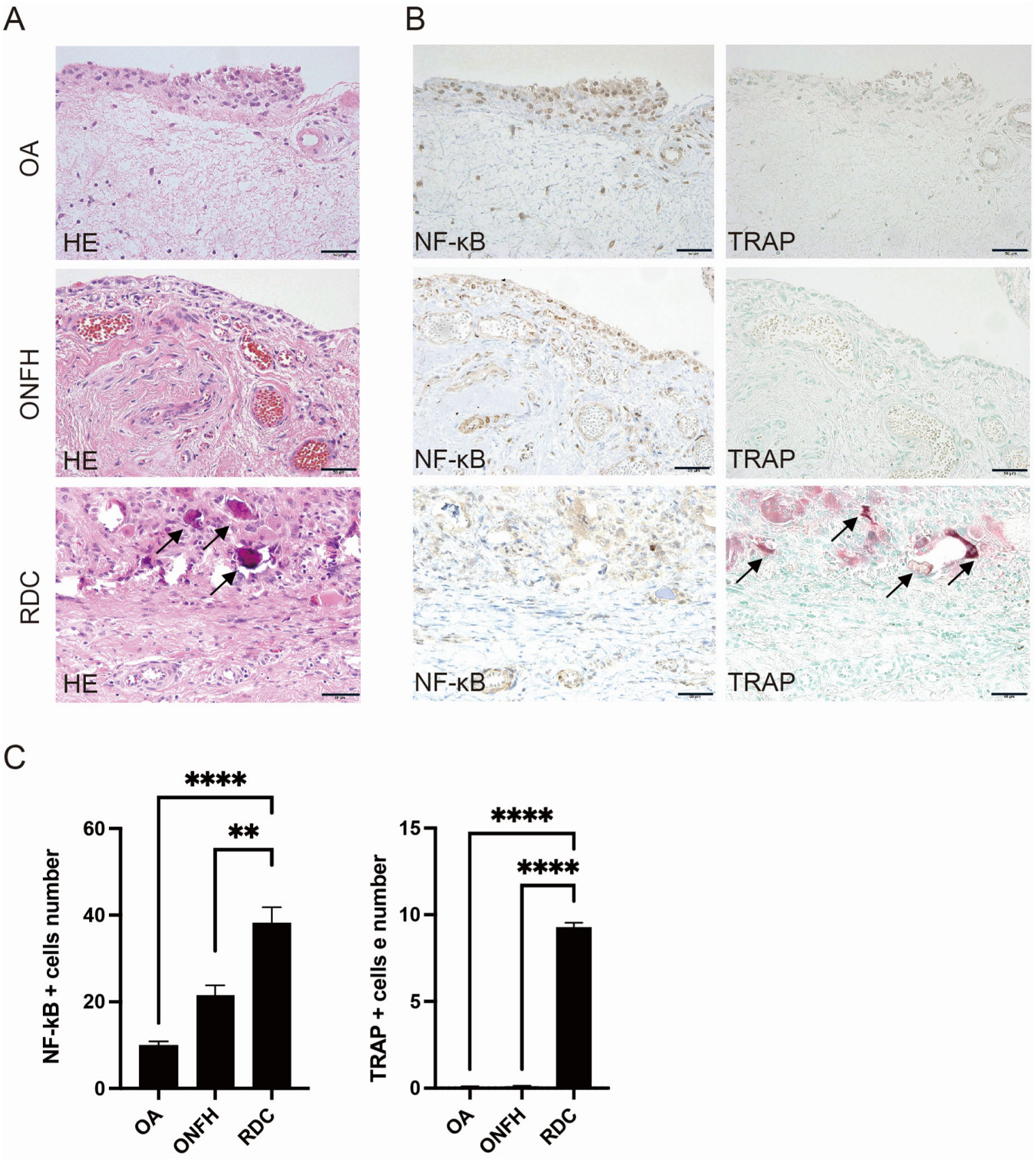
A
B
OA
ONFH
RDC
HE
NF-κB
TRAP
C
NF-kB + cells number
TRAP + cells e number
****
**
****
****
0
20
40
60
0
5
10
15
OA
ONFH
RDC

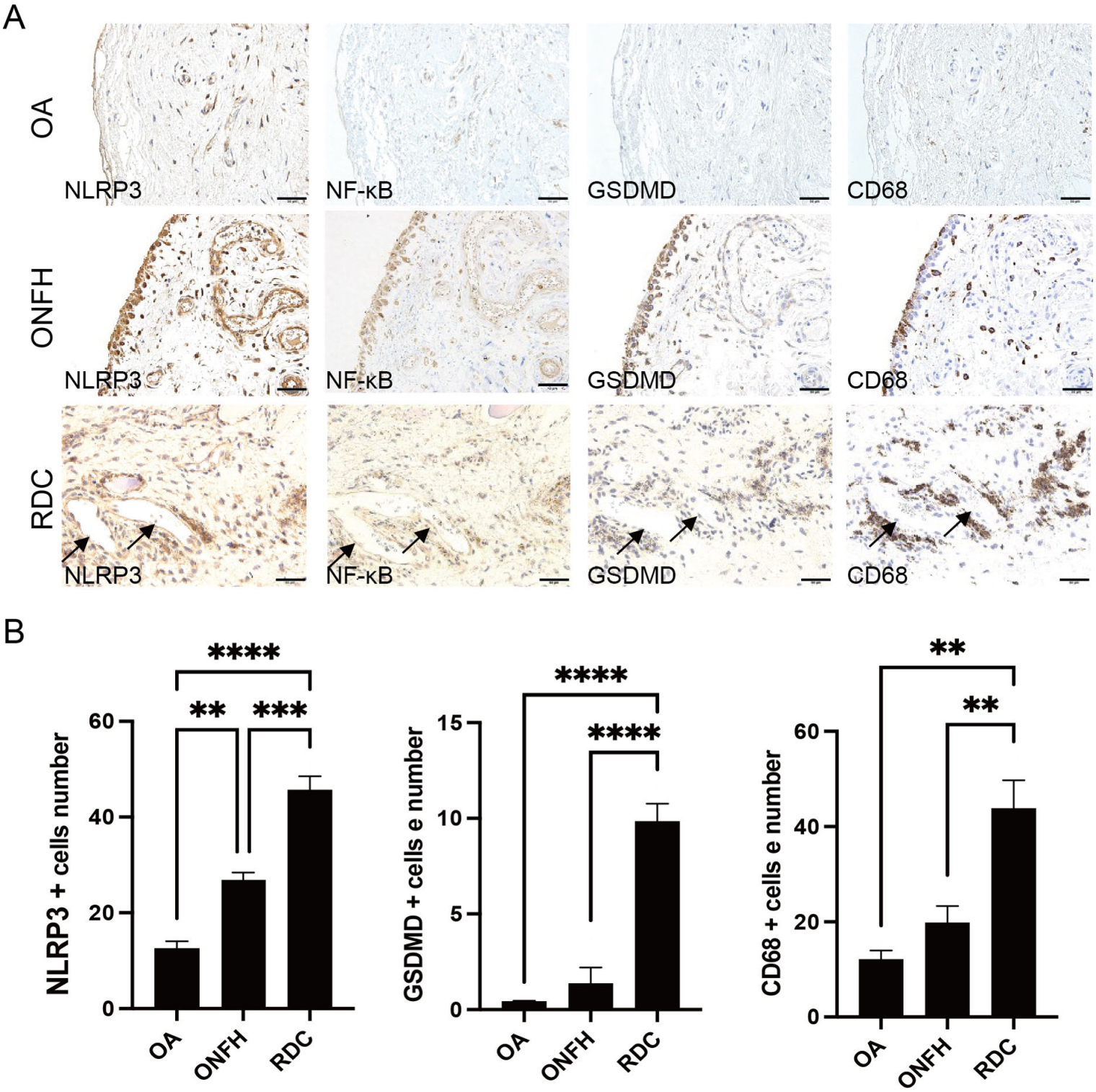
A
OA
ONFH
RDC
NLRP3
NF-κB
GSDMD
CD68
B
NLRP3 + cells number
GSDMD + cells e number
CD68 + cells e number
OA
ONFH
RDC
****
**
***
****
****
**
**

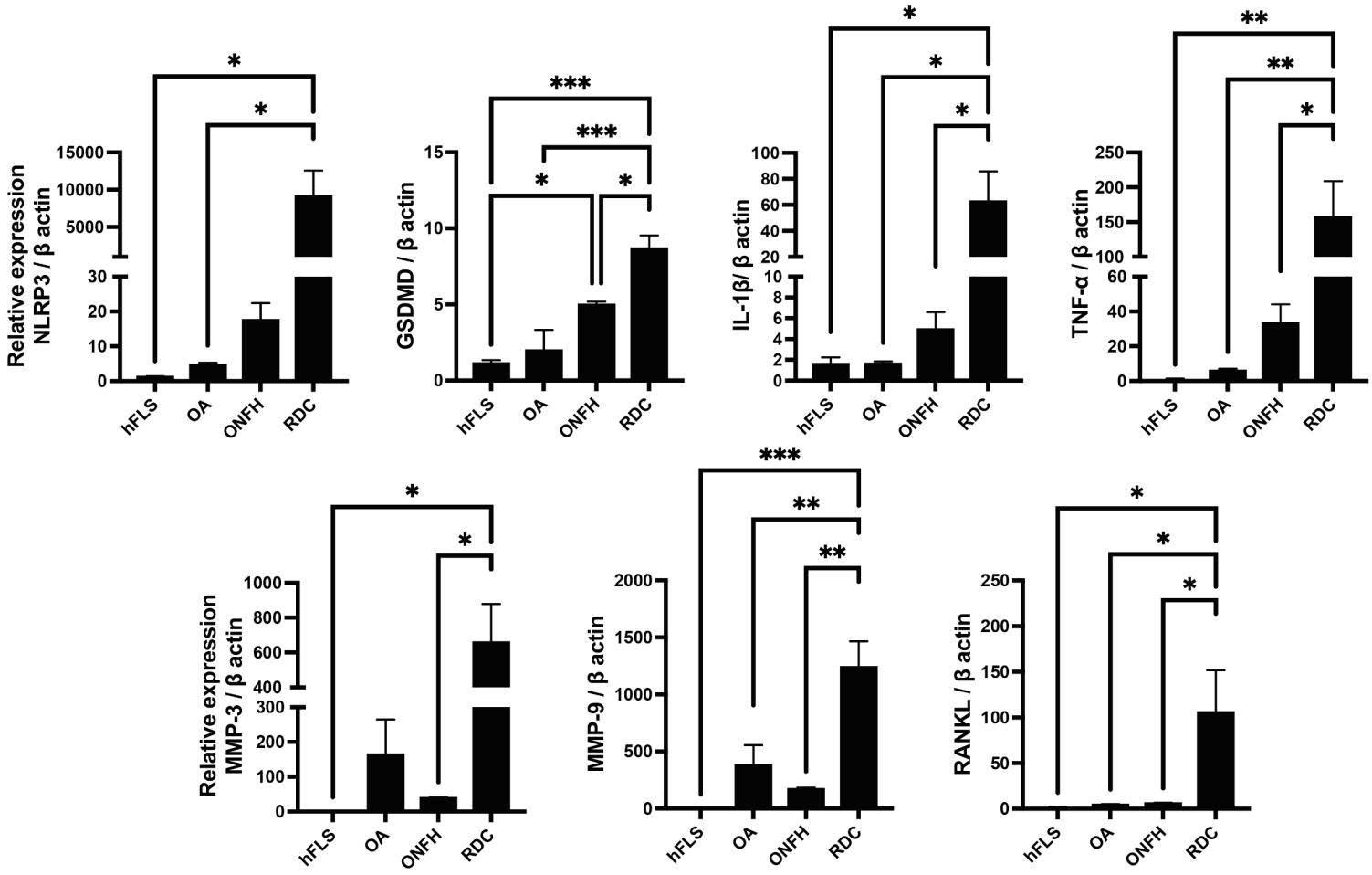
Relative expression NLRP3 / β actin
GSDMD / β actin
IL-1β/ β actin
TNF-α / β actin
Relative expression MMP-3 / β actin
MMP-9 / β actin
RANKL / β actin
hFLS
OA
ONFH
RDC

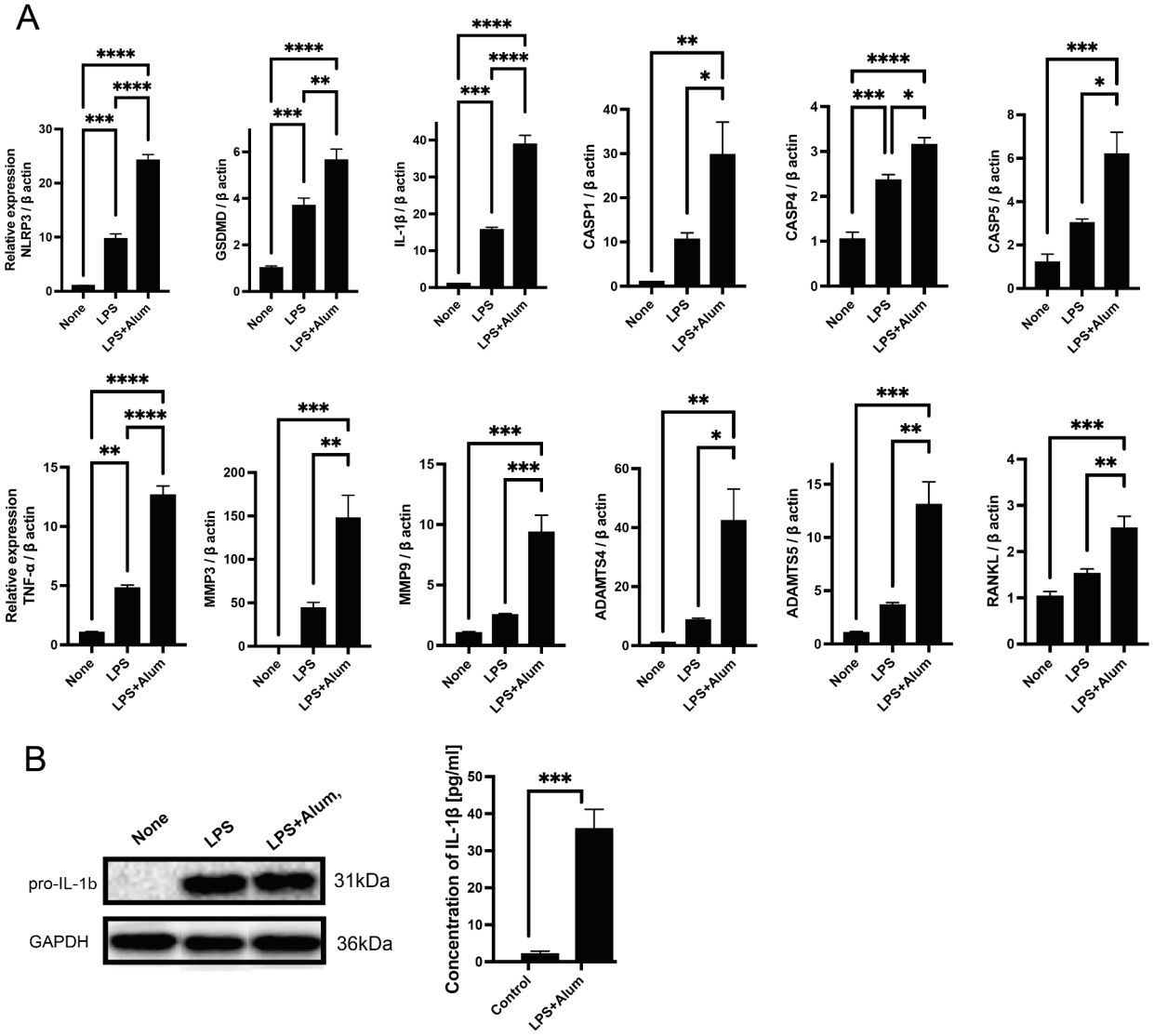
A
Relative expression NLRP3 / β actin
GSDMD / β actin
IL-1β / β actin
CASP1 / β actin
CASP4 / β actin
CASP5 / β actin
Relative expression TNF-α / β actin
MMP3 / β actin
MMP9 / β actin
ADAMTS4 / β actin
ADAMTS5 / β actin
RANKL / β actin
None
LPS
LPS+Alum
B
None
LPS
LPS+Alum,
pro-IL-1b
31kDa
GAPDH
36kDa
Concentration of IL-1β [pg/ml]
Control
LPS+Alum

A

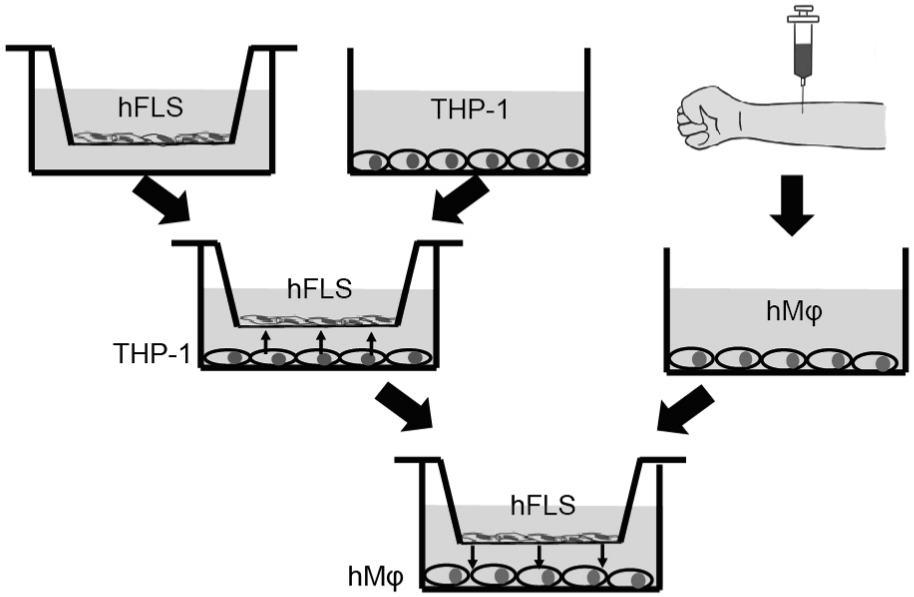
hFLS
THP-1
hFLS
THP-1
hMφ
hFLS
hMφ

B

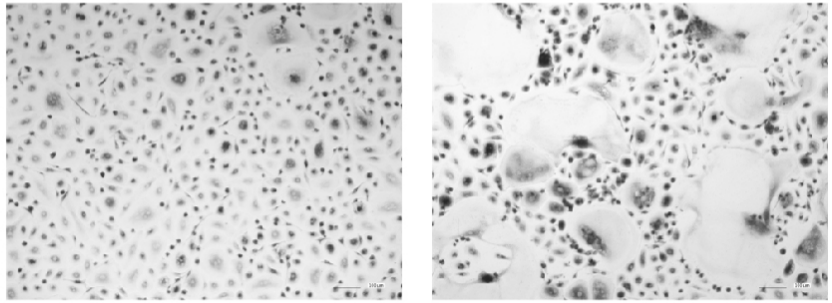
Non-stimulation
LPS + Alum

C

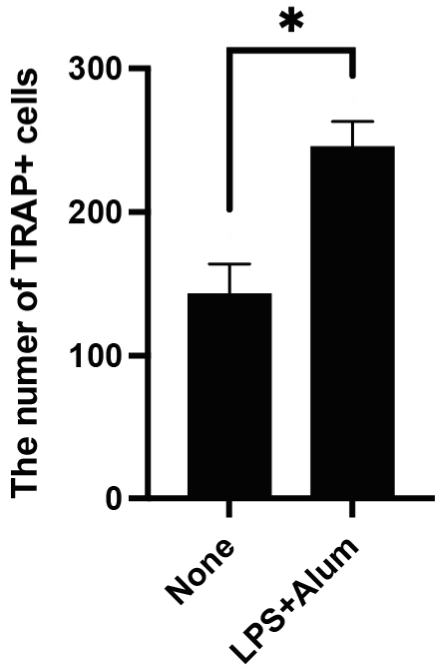
*
300
200
100
0
The numer of TRAP+ cells
None
LPS+Alum